Available online at www.sciencedirect.com
SCIENCE DIRECT®
Chaos, Solitons and Fractals 20 (2004) 503–521
CHAOS
SOLITONS & FRACTALS
www.elsevier.com/locate/chaos

Anti-control of chaos of two-degrees-of-freedom loudspeaker system and chaos synchronization of different order systems

Z.-M. Ge *, W.-Y. Leu

Department of Mechanical Engineering, National Chiao Tung University, 1001 Ta Hsueh Road, Hsinchu 300, Taiwan, ROC

Accepted 23 July 2003

Abstract

The chaos anti-control and synchronization of a two-degrees-of-freedom loudspeaker system are studied in this paper. Anti-control term is added to change state from regular to chaos. The anti-control methods such as addition of a constant force, of a periodic square wave, of a periodic saw tooth wave, of a periodic triangle wave, of a periodic rectified sinusoidal wave and of the $x|x|$ term are used. The results are illustrated by numerical results, i.e. bifurcation diagram and Lyapunov exponents. Next, chaos synchronization of different order system is studied. Two methods are presented to achieve the synchronization: the addition of the coupling terms, the linearization of the error dynamics. The results are illustrated by phase diagram and time response.

1. Introduction

Lorenz studied the strange changes in the atmosphere which is the first example to study chaos in 1963. In the past four decades, a large number of studies have shown that chaotic phenomena are observed in many physical systems that possess non-linearity [1,2]. It was also reported that the chaotic motion occurred in many non-linear control systems [3].

Furthermore, the problem of anti-controlling chaos (from periodic to chaotic) is interesting, non-traditional, and indeed very challenging. More importantly, within the biological context, anti-control of chaos suggests great potential for future applications. Recently, there have been many successful papers towards the goal of anti-control, which are essentially experimental or semi-analytical [4].

In this paper, chaos anti-control and synchronization of a two-degrees-of-freedom loudspeaker system are researched by many methods. First, a two- degrees-of-freedom loudspeaker system model and states equations of motion for it are introduced. Next, the bifurcation diagram and the Lyapunov exponent are expressed by numerical analysis.

Then, anti-control of chaos is applied by adding different kinds of external forces. The external forces are a constant force, a periodic square wave, a periodic saw tooth wave, a periodic triangle wave, a periodic rectified sin and $x|x|$ term. The results are demonstrated by various numerical results.

Chaos synchronization of different order systems are studied in Section 4. First, synchronization of two degrees-of-freedom loudspeaker system and Chua system is achieved by application of unidirectional coupled term. Next, synchronization of two-degrees-of-freedom loudspeaker system and Duffing system is discussed by application of the linearization of the error dynamics.

Finally, the conclusion of the whole paper is briefly stated.

* Corresponding author. Tel.: +886-35712121; fax: +886-35720634.
E-mail address: zmg@cc.nctu.edu.tw (Z.-M. Ge).

0960-0779/$ - see front matter © 2003 Elsevier Ltd. All rights reserved.
doi:10.1016/j.chaos.2003.07.001

2. Equations of motion

The loudspeaker system considered here is depicted in Fig. 1. It is a loudspeaker system having two-degrees-of-freedom, where one is the electric charge on the capacitor plate and the other is displacement of the parallel plate capacitor.

The state equations of loudspeaker system are described by [5]

$$\begin{cases} \dot{x}_1 = x_2 \\ \dot{x}_2 = -a_{21}x_1 - a_{22}x_2 + a_{23}x_3 + a_{24}x_3^2 + a_{25}\sin\left(\frac{\omega}{\Omega}\right)\tau \\ \dot{x}_3 = x_4 \\ \dot{x}_4 = a_{41}x_1 + a_{42}x_1x_3 - a_{43}x_3 - a_{44}x_4 \end{cases} \tag{2.1}$$

where $a_{21} = 1$, $a_{22} = 0.05$, $a_{23} = 2$, $a_{24} = 0.0847$, $a_{25} = \frac{A}{mx_0\Omega^2}$, $a_{41} = 0.0694$, $a_{42} = 0.0694$, $a_{43} = 1.27$, $a_{44} = 0.5$.

The bifurcation diagram of the loudspeaker system is depicted in Fig. 2. The range of A is $[38, 44]$ with the incremental value 0.01. Lyapunov exponents of loudspeaker system are plotted in Fig. 3.

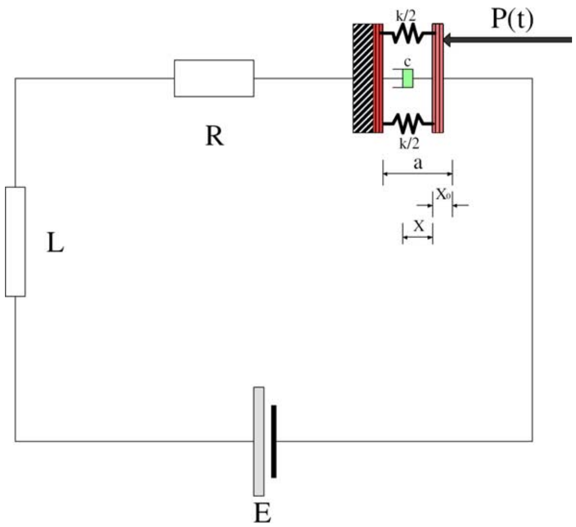

Fig. 1. A schematic diagram of loudspeaker system.

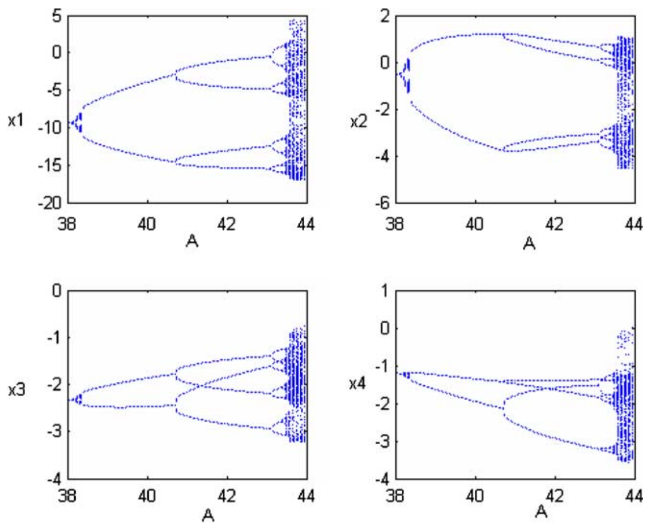

Fig. 2. Bifurcation diagram for A between 38 and 44.

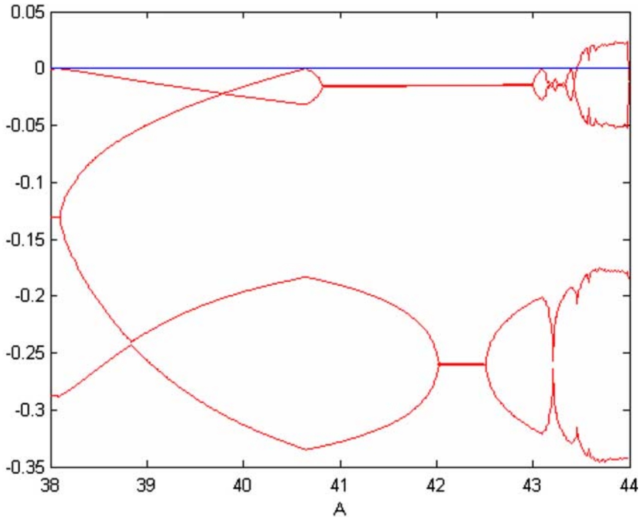

Fig. 3. The Lyapunov exponent for A between 38 and 44.

3. Anti-control of chaos

Creating chaos is called anti-control of chaos at times [6]. The problem of anti-control of chaos is interesting, non-traditional, and indeed very challenging.

In this section, many methods of anti-control, such as addition of a constant force, of a periodic square wave, of a periodic saw tooth wave, of a periodic triangle wave, of a periodic rectified sinusoidal wave and of a $x|x|$ term [7], are proposed, which can enhance the existing chaos of the originally chaotic system. The results are demonstrated by numerical results, i.e. bifurcation diagram and Lyapunov exponent.

3.1. Anti-control of chaos by addition of a constant force

One can add a constant term to control the system dynamics from periodic motion to chaotic motion in non-linear non-autonomous system. This process is called anti-control. It ensures effective controlling in a simple way by choosing the value of the force. The constant force F_c is applied on the plate of the capacitor. Thus Eq. (2.1) becomes

$$\begin{cases} \dot{x}_1 = x_2 \\ \dot{x}_2 = -a_{21}x_1 - a_{22}x_2 + a_{23}x_3 + a_{24}x_3^2 + a_{25}\sin\left(\frac{\omega}{\Omega}\right)\tau + F_c \\ \dot{x}_3 = x_4 \\ \dot{x}_4 = a_{41}x_1 + a_{42}x_1x_3 - a_{43}x_3 - a_{44}x_4 \end{cases} \tag{3.1.1}$$

Changing the force F_c from zero downwards, the chaotic behavior is increased when $F_c = -0.35, -1$. Bifurcation diagram and corresponding Lyapunov exponent diagram are shown as Figs. 4–6. The spectral analysis of the Lyapunov exponent diagram has been proved to be the most useful dynamic diagnostic tool for checking chaotic motion.

3.2. Anti-control of chaos by addition of a periodic force

Another way to anti-control chaos is using a periodic force as a control force. For this purpose, the added periodic force F_p is applied on the plate of the capacitor. Eq. (2.1) becomes

$$\begin{cases} \dot{x}_1 = x_2 \\ \dot{x}_2 = -a_{21}x_1 - a_{22}x_2 + a_{23}x_3 + a_{24}x_3^2 + a_{25}\sin\left(\frac{\omega}{\Omega}\right)\tau + F_p \\ \dot{x}_3 = x_4 \\ \dot{x}_4 = a_{41}x_1 + a_{42}x_1x_3 - a_{43}x_3 - a_{44}x_4 \end{cases} \tag{3.2.1}$$

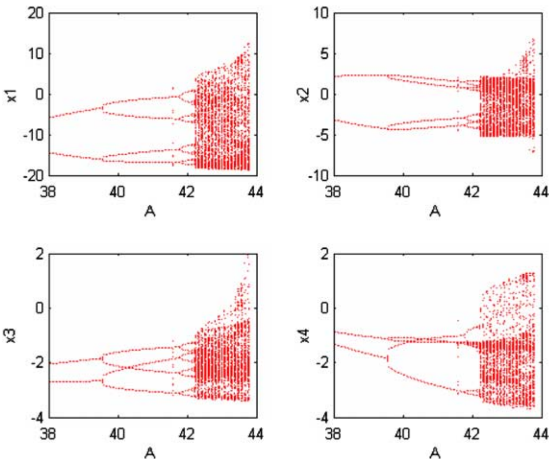

Fig. 4. Bifurcation diagram for A between 38 and 44, $F_c = -0.35$.

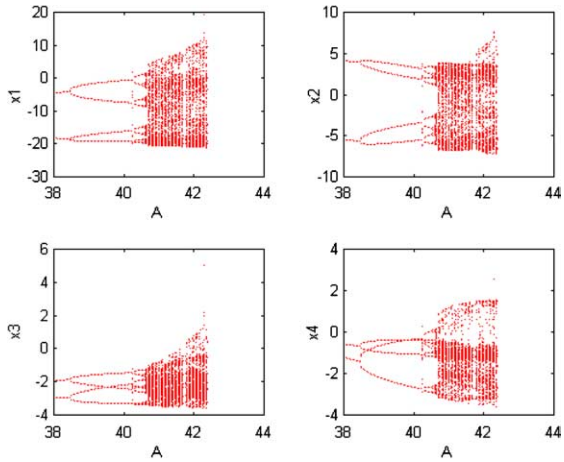

Fig. 5. The bifurcation diagram for A between 38 and 44, $F_c = -1$.

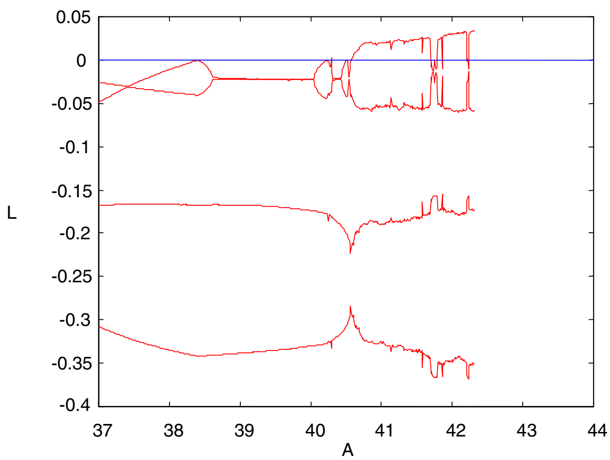

Fig. 6. The Lyapunov exponent diagram for A between 38 and 44, $F_c = -1$.

3.2.1. Adding a periodic force of square wave

In Eq. (3.2.1) periodic force F_p is a square wave. The square wave form is described by

$$F_p(t) = \sum_{k=0}^{\infty}[(-1)^k \cdot A \cdot u(t-\tau)] \tag{3.2.2}$$

where A is the amplitude of the square wave, $\tau = k\frac{P}{2}$, P is the period of the square wave, $u(t)$ is a unit step function.

The parameters of the periodic force are chosen such that amplitude A varies for fixed period P or the period varies with fixed amplitude. The chaotic behavior is effectively increased. Bifurcation diagram is shown as Figs. 7–9.

3.2.2. Adding a periodic force of saw tooth wave

In Eq. (3.2.1) periodic force F_p is a saw tooth wave. The saw tooth wave form is described by

$$F_p(t) = \frac{A}{P}t - A \cdot \sum_{k=1}^{\infty}[u(t-\tau)] \tag{3.2.3}$$

where A is the amplitude of the saw tooth wave, $\tau = kP$, P is the period of the saw tooth wave, $u(t)$ is a unit step function.

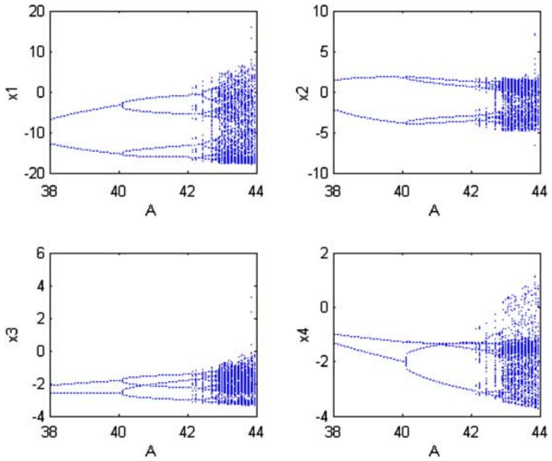

Fig. 7. Bifurcation diagram for A between 38 and 44, the parameter of square wave chosen as $P = 0.5$, $A = -0.4$.

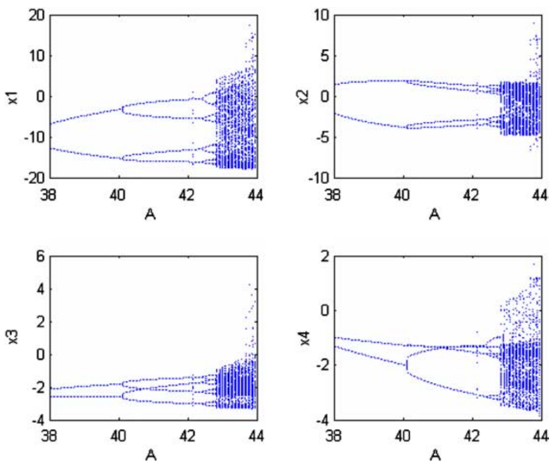

Fig. 8. Bifurcation diagram for A between 38 and 44, the parameter of square wave chosen as $P = 1$, $A = -0.4$.

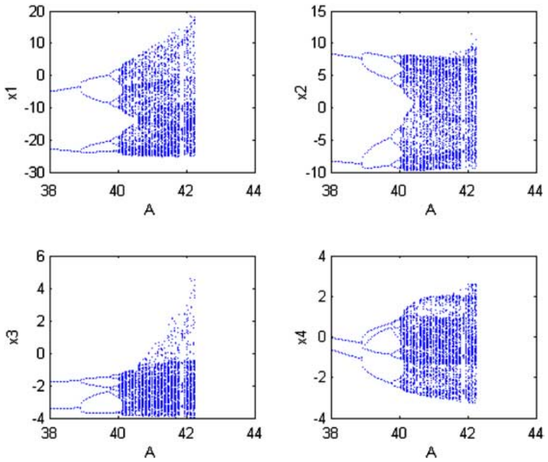

Fig. 9. Bifurcation diagram for A between 38 and 44, the parameter of square wave chosen as $P = 1$, $A = -4$.

The parameters of the periodic force are chosen such that amplitude A varies for fixed period P. The chaotic behavior is effectively increased. Bifurcation diagram is shown as Figs. 10 and 11.

3.2.3. Adding a periodic force of triangle wave

In Eq. (3.2.1) periodic force F_p is a triangle wave. The triangle wave form is described by

$$F_p(t) = \frac{A}{2} - \frac{16A}{\pi^2} \sum_{k=0}^{\infty} \left(\frac{1}{(2+4k)^2} \cos \frac{2\pi}{P} t \right) \tag{3.2.4}$$

where A is the amplitude of the triangle wave, P is the period of the triangle wave.

The parameters of the periodic force are chosen such that amplitude A varies for fixed period P or the period varies with fixed amplitude. The chaotic behavior is effectively increased. Bifurcation diagram is shown as Figs. 12–14.

3.2.4. Adding a periodic force of rectified sinusoidal wave

In Eq. (3.2.1) periodic force F_p is a rectified sinusoidal wave. The rectified sinusoidal wave form is described by

$$F_p = A|\sin(\omega t)| \tag{3.2.5}$$

where A is the amplitude of the rectified sinusoidal wave, $P = \frac{\pi}{\omega}$, P is the period of the rectified sinusoidal wave,

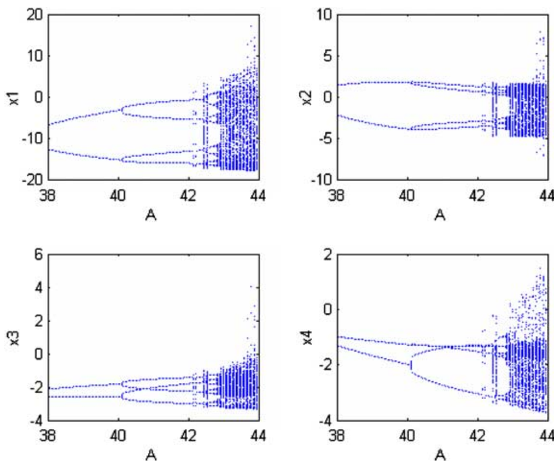

Fig. 10. Bifurcation diagram for A between 38 and 44, the parameter of saw tooth wave chosen as $P = 0.5$, $A = -0.4$.

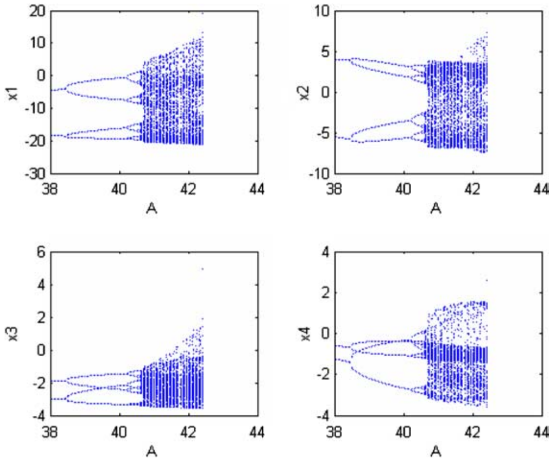

Fig. 11. Bifurcation diagram for A between 38 and 44, the parameter of saw tooth wave chosen as $P = 0.5$, $A = -2$.

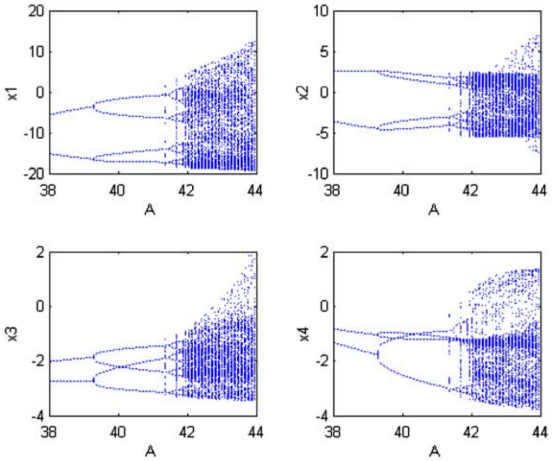

Fig. 12. Bifurcation diagram for A between 38 and 44, the parameter of triangle wave chosen as $P = 0.5$, $A = -1$.

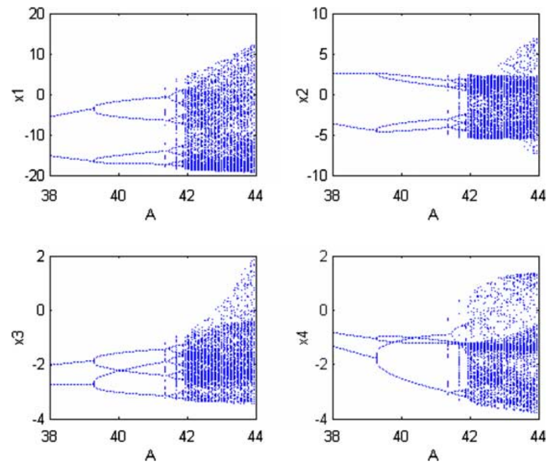

Fig. 13. Bifurcation diagram for A between 38 and 44, the parameter of triangle wave chosen as $P = 1$, $A = -1$.

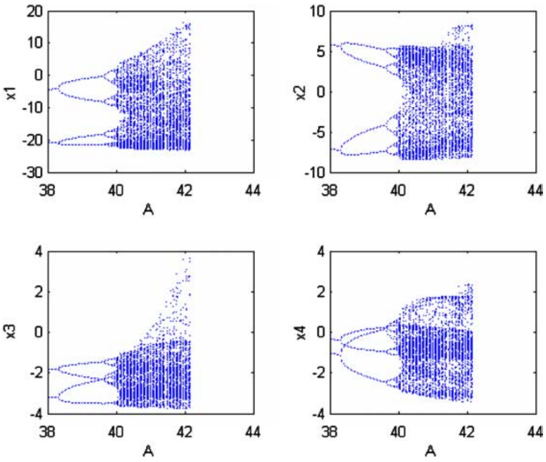

Fig. 14. Bifurcation diagram for A between 38 and 44, the parameter of triangle wave chosen as $P = 1$, $A = -3$.

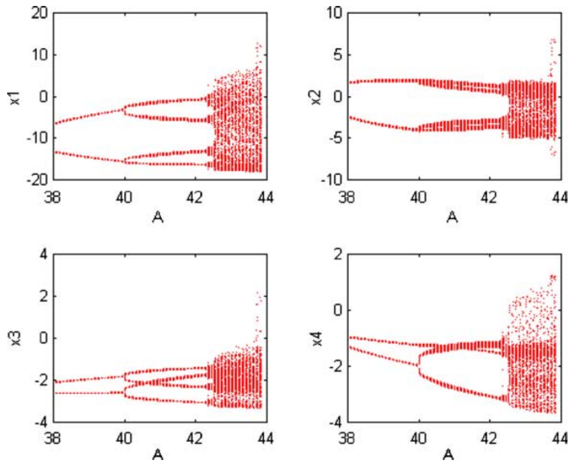

Fig. 15. Bifurcation diagram for A between 38 and 44, the parameter of rectified sinusoidal wave chosen as $P = 1$, $A = -0.4$.

The parameters of the periodic force are chosen such that amplitude A varies for fixed frequency P or the frequency varies with fixed amplitude. The chaotic behavior is effectively increased. Bifurcation diagram is shown as Figs. 15–17.

3.3. Anti-control of chaos by addition of a $x|x|$ term

We add $k_2x_2|x_2|$ to the second equation of Eq. (2.1) where k_2 is the strength. Bifurcation diagrams are shown as Fig. 18. We add $k_4x_4|x_4|$ to the fourth equation of Eq. (2.1) where k_4 is the strength. Bifurcation diagrams are shown as Fig. 19. We add $k_1x_1|x_1|$, $k_2x_2|x_2|$ and $k_4x_4|x_4|$ to the first equation, second equation and fourth equation of Eq. (2.1), respectively, where k_1, k_2 and k_4 are the strengths. Bifurcation diagrams are shown as Fig. 20.

4. Chaos synchronization of different order systems

The chaos synchronization of different order systems is discussed in this section. Two kinds of methods to achieve the synchronization are presented: the addition of the coupling terms and the linearization of the error dynamics.

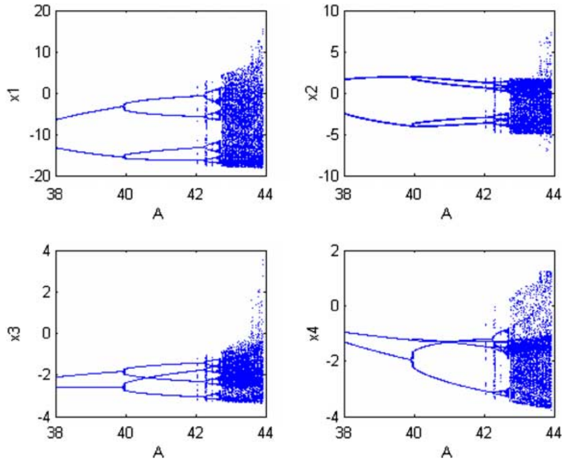

Fig. 16. Bifurcation diagram for A between 38 and 44, the parameter of rectified sinusoidal wave chosen as $P = 0.5$, $A = -0.4$.

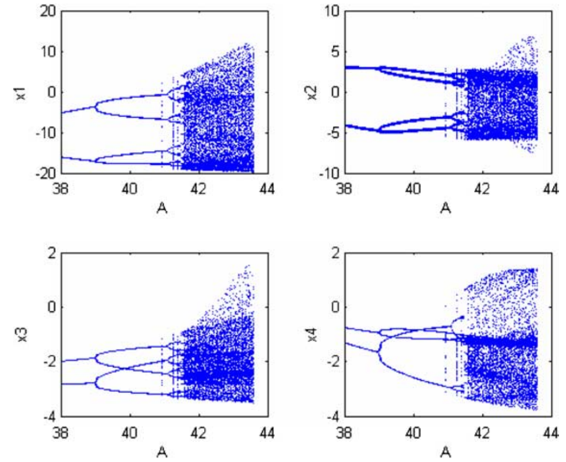

Fig. 17. Bifurcation diagram for A between 38 and 44, the parameter of rectified sinusoidal wave chosen as $P = 0.5$, $A = -1$.

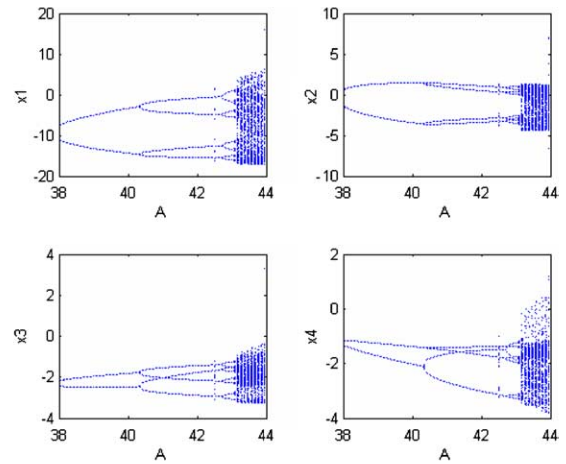

Fig. 18. Bifurcation diagram for A between 38 and 44, where $k_2 = 0.0002$.

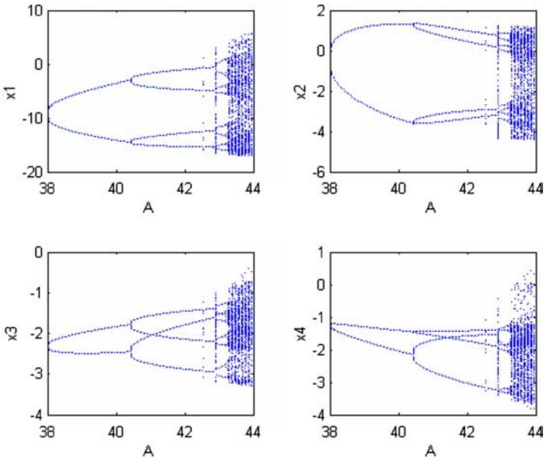

Fig. 19. Bifurcation diagram for A between 38 and 44, where $k_4 = 0.0015$.

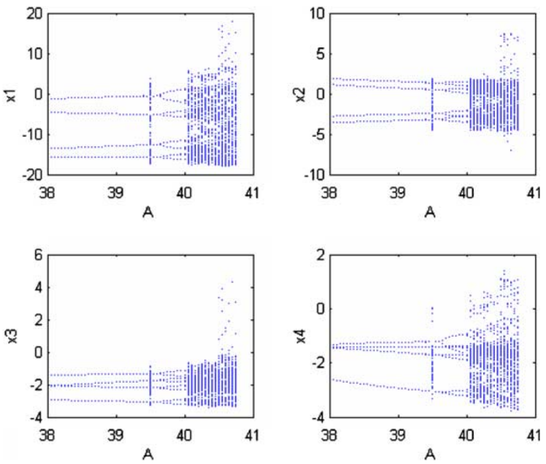

Fig. 20. Bifurcation diagram for A between 38 and 44, where $k_1 = 0.0015$, $k_2 = 0.00015$, $k_4 = 0.0015$.

4.1. Chaos synchronization of different order coupled chaotic systems

The chaotic synchronization of fourth-order response systems and third-order drive oscillator is studied in this section.

Eq. (2.1) is as follows

$$\begin{cases} \dot{x}_1 = x_2 \\ \dot{x}_2 = -a_{21}x_1 - a_{22}x_2 + a_{23}x_3 + a_{24}x_3^2 + a_{25}\sin\left(\frac{\omega}{\Omega}\right)\tau \\ \dot{x}_3 = x_4 \\ \dot{x}_4 = a_{41}x_1 + a_{42}x_1x_3 - a_{43}x_3 - a_{44}x_4 \end{cases} \tag{4.1.1}$$

The parameters are chosen as follows: $a_{21} = 1$, $a_{22} = 0.05$, $a_{23} = 2$, $a_{24} = 0.0847$, $a_{25} = 5.5652$, $a_{41} = 0.0694$, $a_{42} = 0.0694$, $a_{43} = 1.27$, $a_{44} = 0.5$.

Chua system is an electronic circuit with one non-linear resistive element. The circuit equations can be written as a third-order system that is given by the following dimensionless form [8]

$$\begin{aligned} \dot{y}_1 &= \gamma_1[-y_1 + y_2 - f(y_1)] \\ \dot{y}_2 &= y_1 - y_2 + y_3 \\ \dot{y}_3 &= -\gamma_2 y_2 \end{aligned} \tag{4.1.2}$$

where $f(y_1) = \gamma_3 y_1 + 0.5(\gamma_4 - \gamma_3)[|y_1 + 1| - |y_1 - 1|]$, γ_i, $i = 1, 2, 3, 4$, are positive constants. Let us take system Eq. (4.1.2) as the drive system. The parameters are chosen as follows: $r = 10.0$, $r_2 = 14.87$, $r_3 = -0.68$, $r_4 = -1.27$. Initial condition is arbitrarily located at the point $y(0) = (0.1, -0.5, 0.2)$.

The coupled chaotic systems is presented by adding linear coupling term $D(x_2 - y_2)$ on the second equation of Eq. (4.1.2) as

$$\begin{aligned} \dot{y}_1 &= \gamma_1[-y_1 + y_2 - f(y_1)] \\ \dot{y}_2 &= y_1 - y_2 + y_3 + D(x_2 - y_2) \\ \dot{y}_3 &= -\gamma_2 y_2 \end{aligned} \tag{4.1.3}$$

where D is coupling strength. When $D = 10,000$, the system will be synchronized and the result is shown in Fig. 21.

4.2. Chaos synchronization of different order systems by linearization of error dynamics

The chaotic synchronization of a fourth-order loudspeaker drive system and a second-order Duffing response oscillator is studied in this section.

It is shown that dynamical evolution of the second-order response oscillators can be synchronized with the canonical projection of the fourth-order chaotic system. In this sense, it is said that synchronization is achieved in reduced order. Duffing equation is chosen as response system whereas loudspeaker system equation is defined as drive system. The synchronization scheme has non-linear feedback structure. The loudspeaker system Eq. (2.1) is

$$\begin{cases} \dot{x}_1 = x_2 \\ \dot{x}_2 = -a_{21}x_1 - a_{22}x_2 + a_{23}x_3 + a_{24}x_3^2 + a_{25}\sin\left(\frac{\omega}{\Omega}\right)\tau \\ \dot{x}_3 = x_4 \\ \dot{x}_4 = a_{41}x_1 + a_{42}x_1x_3 - a_{43}x_3 - a_{44}x_4 \end{cases} \tag{4.2.1}$$

The parameters are chosen as follows: $a_{21} = 1$, $a_{22} = 0.05$, $a_{23} = 2$, $a_{24} = 0.0847$, $a_{25} = 5.5652$, $a_{41} = 0.0694$, $a_{42} = 0.0694$, $a_{43} = 1.27$, $a_{44} = 0.5$. The chaotic phase portrait is shown as Fig. 22.

Now let us consider the Duffing equation, which is given by

$$\begin{cases} \dot{y}_1 = y_2 \\ \dot{y}_2 = y_1 - y_1^3 - \delta y_2 + \tau_e(\tau) + u \end{cases} \tag{4.2.2}$$

where δ is a positive parameter that represents damping coefficient, $\tau_e(\tau) = \alpha\cos(\omega\tau)$ denotes driving force and u is the coupling force (controller), parameters are chosen as $\delta = 0.15$, $\alpha = 0.3$, and $\omega = 1.0$. Initial condition is arbitrarily located at the point $y(0) = (0, 0)$. The phase portrait s is shown as Fig. 23.

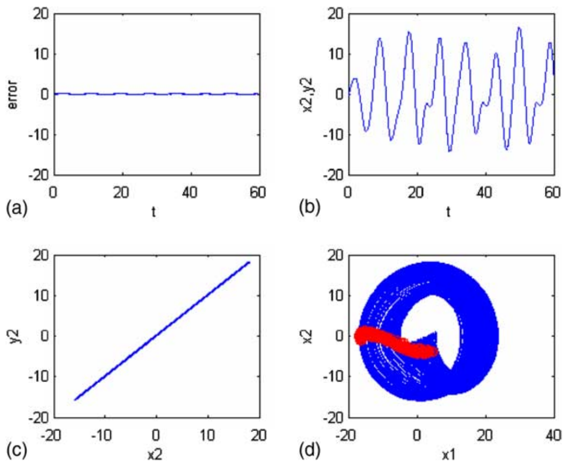

Fig. 21. (a) Time history of error, (b) time history of x_2 (solid line) and y_2 (dotted line) and (c, d) phase portraits of the synchronization system for $D = 10,000$.

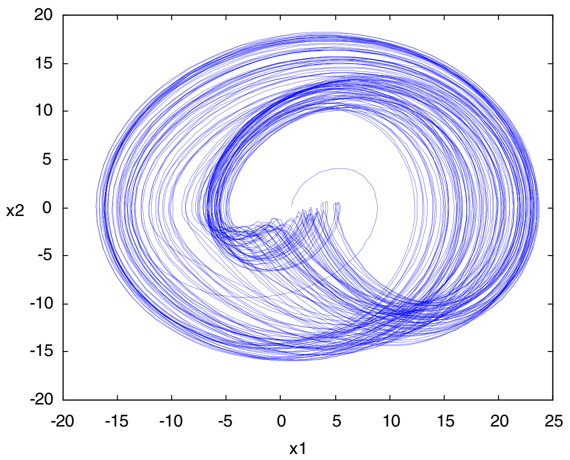

Fig. 22. Phase portrait of the loudspeaker system without control term.

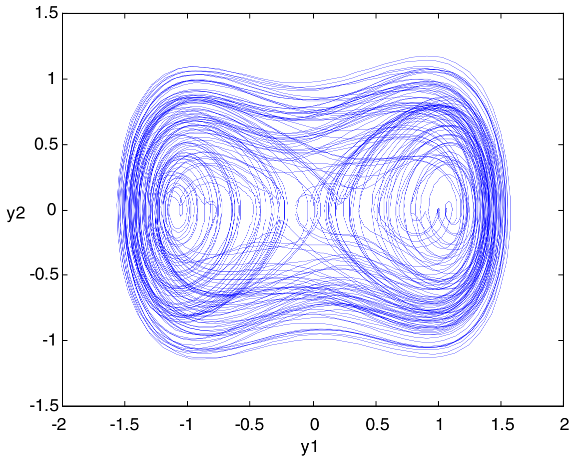

Fig. 23. Phase portrait of the Duffing equation without control term.

The differences between the states of the drive system and response system are $e_1 = y_1 - x_1$, $e_2 = y_2 - x_2$. The figures are shown as Figs. 24 and 25.

Then the error dynamics is

$$\begin{cases} \dot{e}_1 = e_2 \\ \dot{e}_2 = e_1 - \delta e_2 + \tau'_e + u \end{cases} \tag{4.2.3}$$

where

$$\tau'_e = -[(a_{23} + a_{24}x_3)x_3 + a_{25}\sin(\varpi/\Omega)\tau - \alpha\cos(w\tau) - (1 + a_{21} - y_1^2)y_1 - (a_{22} - \delta)y_2]$$

Let $u = -\tau'_e + k_1e_1 + k_2e_2$.

Linearization of Eq. (4.2.3) becomes

$$\begin{cases} \dot{e}_1 = e_2 \\ \dot{e}_2 = -(a_{21} - k_1)e_1 - (a_{22} - k_2)e_2 \end{cases} \tag{4.2.4}$$

i.e.

$$\begin{bmatrix} \dot{e}_1 \\ \dot{e}_2 \end{bmatrix} = \begin{bmatrix} 0 & 1 \\ -(a_{21} - k_1) & -(a_{22} - k_2) \end{bmatrix} \begin{bmatrix} e_1 \\ e_2 \end{bmatrix} \tag{4.2.5}$$

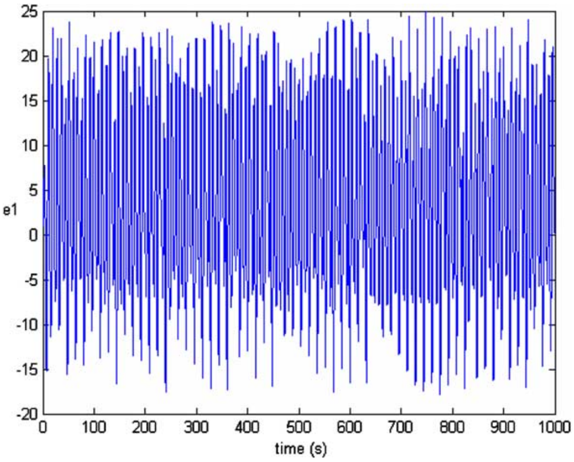

Fig. 24. Time history of error e_1 without control term.

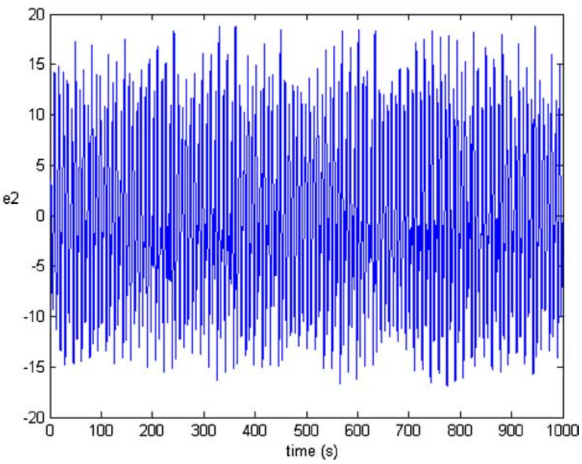

Fig. 25. Time history of error e_2 without control term.

We can rewrite Eq. (4.2.5) as

$$\dot{e} = Ae \tag{4.2.6}$$

The characteristic equation of the system is $|A - \lambda I| = 0$ and λ are the eigenvalues of the system. And so

$$\lambda^2 + (a_{22} - k_2)\lambda + (a_{21} - k_1) = 0 \tag{4.2.7}$$

By the theory of linear system, if the eigenvalues are all negative, $e(t) = e(0)\exp(At)$ will converge. So the eigenvalues are chosen as follows, $\lambda_{1,2} = -32, -32$, such that $k_1 = 1023$, $k_2 = 63.05$.

Then the form of controller is

$$u = (a_{23} + a_{24}x_3)x_3 + a_{25}\sin\left(\frac{\omega}{\Omega}\right)\tau - \alpha\cos(\varpi\tau) - (1 + a_{21} - y_1^2)y_1 + (a_{22} - \delta)y_2 - 1023e_1 - 63.05e_2$$

The phase portraits and errors in the presence of control term are shown in Figs. 26–29.

Another example, Duffing equation is chosen as drive system, whereas loudspeaker system equation is defined as response system. The synchronization scheme has non-linear feedback structure.

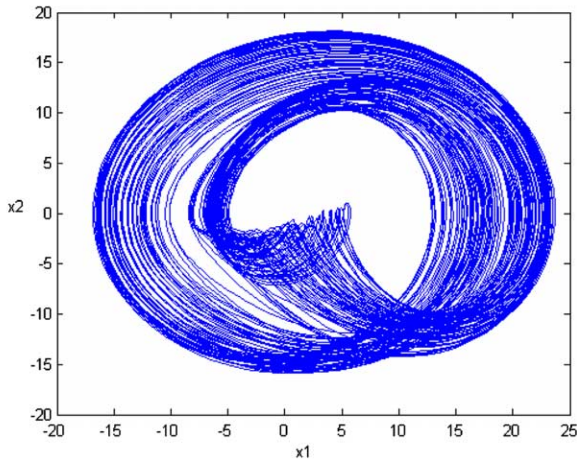

Fig. 26. Phase portrait of the loudspeaker system with control term.

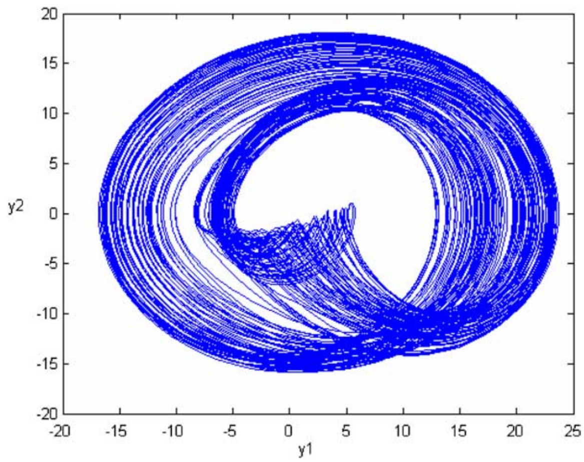

Fig. 27. Phase portrait of the Duffing equation with control term.

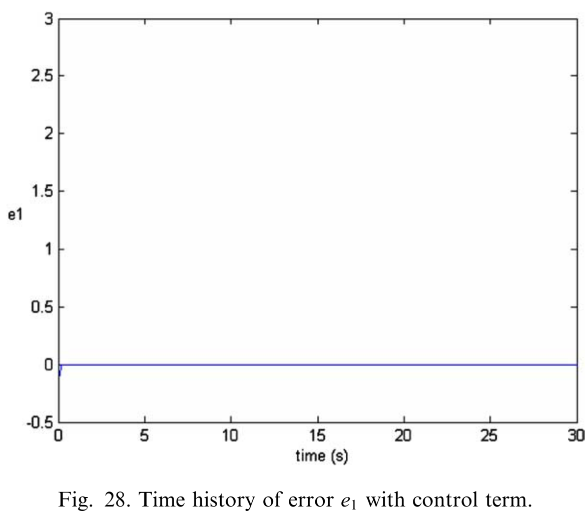

Fig. 28. Time history of error e_1 with control term.

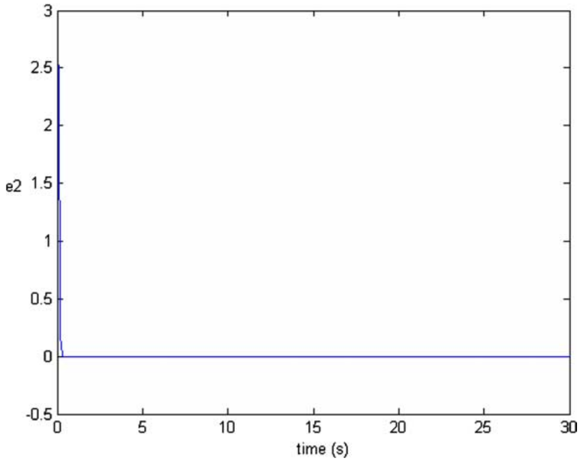

Fig. 29. Time history of error e_2 with control term.

Loudspeaker system Eq. (2.1) becomes

$$\begin{cases} \dot{x}_1 = x_2 \\ \dot{x}_2 = -a_{21}x_1 - a_{22}x_2 + a_{23}x_3 + a_{24}x_3^2 + a_{25}\sin\left(\frac{\omega}{\Omega}\right)\tau + u \\ \dot{x}_3 = x_4 \\ \dot{x}_4 = a_{41}x_1 + a_{42}x_1x_3 - a_{43}x_3 - a_{44}x_4 \end{cases} \tag{4.2.8}$$

The parameters are chosen as follows: $a_{21} = 1$, $a_{22} = 0.05$, $a_{23} = 2$, $a_{24} = 0.0847$, $a_{25} = 5.5652$, $a_{41} = 0.0694$, $a_{42} = 0.0694$, $a_{43} = 1.27$, $a_{44} = 0.5$ and u is the coupling force. The phase portrait is shown as Fig. 30.

Now let us consider the Duffing equation, which is given by

$$\begin{cases} \dot{y}_1 = y_2 \\ \dot{y}_2 = y_1 - y_1^3 - \delta y_2 + \tau_e(\tau) \end{cases} \tag{4.2.9}$$

where δ is a positive parameter which represents damping coefficient, $\tau_e(\tau) = \alpha\cos(\omega\tau)$ denotes driving force.

Parameters are chosen as $\delta = 0.15$, $\alpha = 0.3$, and $\omega = 1.0$. Initial condition is arbitrarily located at the point $y(0) = (0, 0)$. The phase portrait is shown as Fig. 31.

Consider the differences between the states of the drive system and response system are $e_1 = y_1 - x_1$, $e_2 = y_2 - x_2$. Their time histories are shown in Figs. 32 and 33.

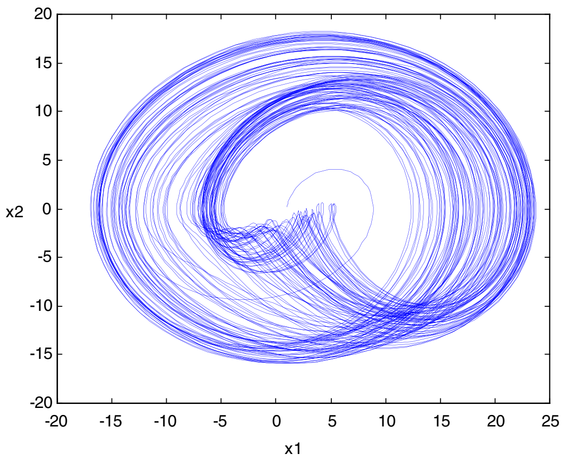

Fig. 30. Phase portrait of the loudspeaker system without control term.

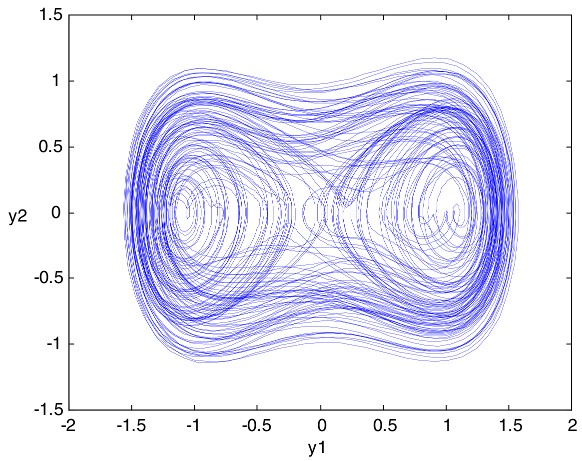

Fig. 31. Phase portrait of the Duffing equation without control term.

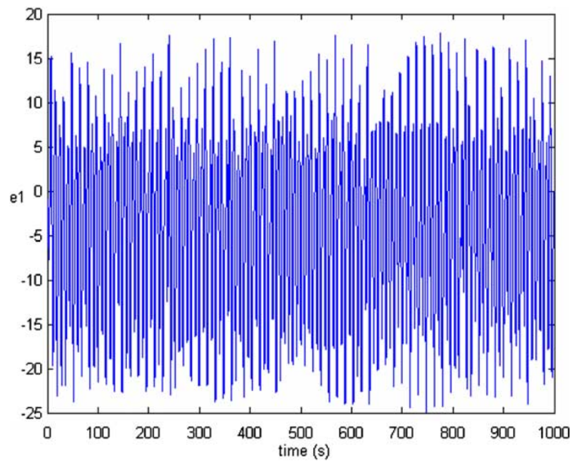

Fig. 32. Time history of error e_1 without control term.

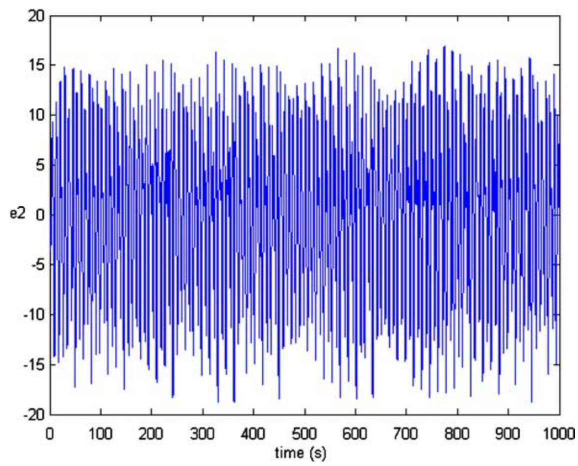

Fig. 33. Time history of error e_2 without control term.

Then the error dynamics is

$$\begin{cases} \dot{e}_1 = e_2 \\ \dot{e}_2 = e_1 - \delta e_2 - \tau_e' - u \end{cases} \tag{4.2.10}$$

where

$$\tau_e' = -[-y_1^3 - a_{25}\sin(\varpi/\Omega)\tau + \alpha\cos(\omega\tau) + (a_{21}+1)x_1 + (a_{22}-\delta)x_2 - (a_{23}+a_{24}x_3)x_3]$$

Let $u = -\tau_e' + k_1 e_1 + k_2 e_2$. Linearization of Eq. (4.2.13) becomes

$$\begin{cases} \dot{e}_1 = e_2 \\ \dot{e}_2 = (1-k_1)e_1 - (\delta + k_2)e_2 \end{cases} \tag{4.2.11}$$

as

$$\begin{bmatrix} \dot{e}_1 \\ \dot{e}_2 \end{bmatrix} = \begin{bmatrix} 0 & 1 \\ (1-k_1) & -(\delta+k_2) \end{bmatrix} \begin{bmatrix} e_1 \\ e_2 \end{bmatrix} \tag{4.2.12}$$

We can rewrite Eq. (4.2.12) as

$$\dot{e} = Ae \tag{4.2.13}$$

The characteristic equation of the system is $|A - \lambda I| = 0$ and λ are the eigenvalues of the system, and so

$$\lambda^2 + (\delta + k_2)\lambda - (1 - k_1) = 0 \tag{4.2.14}$$

By the theory of linear system, if the eigenvalues are all negative, $e(t) = e(0)\exp(At)$ will converge. So the eigenvalues are chosen as follow $\lambda_{1,2} = -29, -29$, such that $k_1 = 842$, $k_2 = 57.85$.

Then the form of controller is

$$u = -y_1^3 - (a_{23} + a_{24}x_3)x_3 - a_{25}\sin\left(\frac{\omega}{\Omega}\right)\tau + \alpha\cos(\varpi\tau) + (a_{21}+1)x_1 + (a_{22}-\delta)x_2 + 842e_1 + 57.85e_2$$

The phase portraits and errors in presence of the control term are shown in Figs. 34–37.

5. Conclusions

In this paper, anti-control and synchronization of a two-degrees-of-freedom loudspeaker system are studied. In Section 2, a two-degrees-of-freedom loudspeaker system model and states equations of motion are introduced. Next, the bifurcation diagram and the Lyapunov exponent are expressed by numerical analysis.

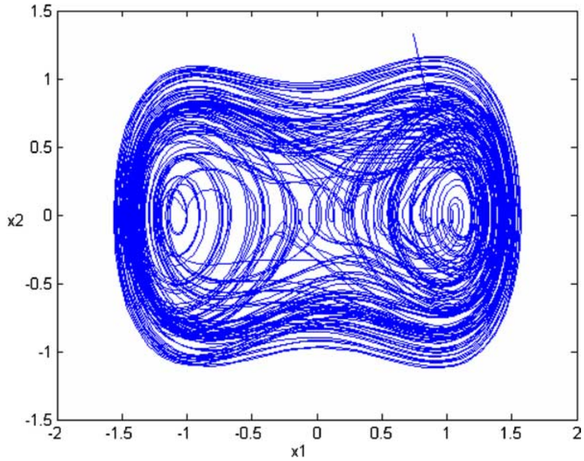

Fig. 34. Phase portrait of the loudspeaker system with control term.

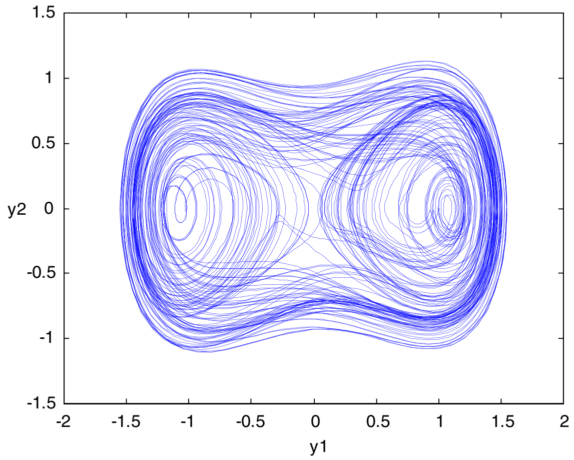

Fig. 35. Phase portrait of the Duffing equation with control term.

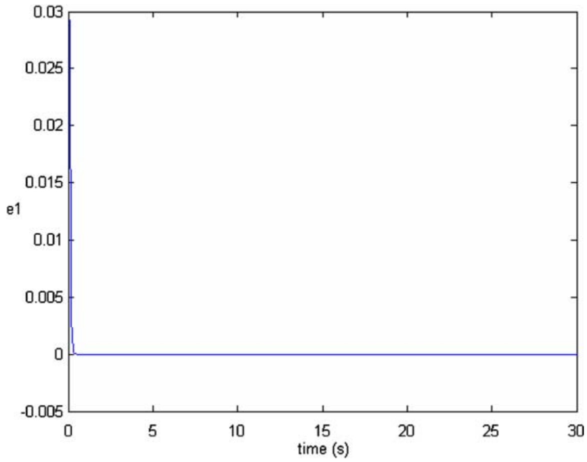

Fig. 36. Time history of error e_1 with control term.

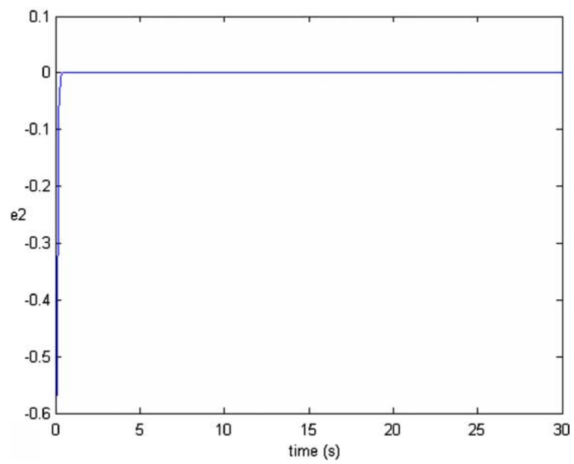

Fig. 37. Time history of error e_2 with control term.

In Section 3, anti-control of chaos is accomplished by adding a constant force, a periodic square wave, a periodic saw tooth wave, a periodic triangle wave, a periodic rectified sinusoidal wave or a $x|x|$ term. The originally existing chaos is enhanced which is illustrated by the bifurcation diagrams and Lyapunov exponents.

The chaos synchronization of different order systems is discussed in the Section 4. First, synchronization of two degrees-of-freedom loudspeaker system and Chua system is achieved by application of unidirectional coupling term, while coupling strength is rather large. Finally, synchronization of two-degrees-of-freedom loudspeaker system and Duffing system is accomplished by application of the linearization of the error dynamics. The results are demonstrated by applying various numerical results.

Acknowledgements

This research was supported by the National Science Council, Republic of China, under grant number NSC 91-2212-E-009-025.

References

[1] Ott E. Chaos in dynamical systems. 2nd ed. England: Cambridge; 2002.
[2] Khailil HK. Nonlinear systems. New Jersey: Prentice-Hall; 2002.
[3] Holmes P. Bifurcation and chaos in a simple feedback control system. In: Proceedings of the IEEE 22nd Conference on Decision and Control, 1983, p. 365–70.
[4] Lai D, Chen G. Distribution of controlled Lyapunov exponents a statistical simulation study. Comput Stat Data Anal 2000;33:69–77.
[5] Ge ZM, Bao TS. Chaos, chaos control and synchronization of electromechanical loudspeaker system. To be published.
[6] Chen G. Control and anticontrol of chaos. In: Proceedings of the 1st International Conference on Control of Oscillations and Chaos, 1997, p. 181–86.
[7] Tang KS, Man KF, Zhong GQ, Chen G. Generating chaos via $x|x$. IEEE Trans Circ Syst 2001;48(5):636–41.
[8] Ricardo F, Gualberto SP. Synchronization of chaotic system with different order. Phys Rev E 2002;65(5):036226-1-7.